THE JOURNAL OF PHYSICAL CHEMISTRY C

Article

pubs.acs.org/JPCC

Engineering of Host–Guest Interactions To Tune the Assembly of Plasmonic Nanoparticles

Dezhi Tan,[†,§] Siyu Tu,[†] Yanqiong Yang,[‡] Sergiy Patskovsky,[†] David Rioux,[†] and Michel Meunier*[,†]

[†]Laser Processing and Plasmonics Laboratory, Department of Engineering Physics, Polytechnique Montréal, Montréal, Québec H3C 3A7, Canada

[‡]Department of Polymer Science and Engineering, Faculty of Materials Science and Chemical Engineering, Ningbo University, Ningbo 315211, People's Republic of China

Supporting Information

ABSTRACT: Controlling the interaction between linking components and nanoobjects is expected to offer exciting new opportunities to induce tunable assembly and modulate the topology and properties of nanostructures. In this work, engineering the exclusive and inclusive host–guest interaction between cucurbit[*n*]urils and salts is demonstrated as a novel strategy to simultaneously realize tunable assembly of plasmonic nanoparticles (NPs) with controllable size and composition and manipulate the stability of the assemblies. As a proof of concept, one-dimensional nanochains of gold, silver, and their alloys with rigid subnanometer interparticle separation and widely tunable optical properties are generated. These exhibit strong dipole coupling between the plasmonic NPs, confirmed by experiments and theoretical simulations. This controllable assembly principle will lead to significant interest not only in supramolecular chemistry and the interactions between supramolecular and plasmonic NPs but also in interaction mechanisms and light management and light harvesting in advanced applications. It is also expected that our approach will be applicable to a wide range of NPs beyond plasmonic NPs with varied sizes and compositions.

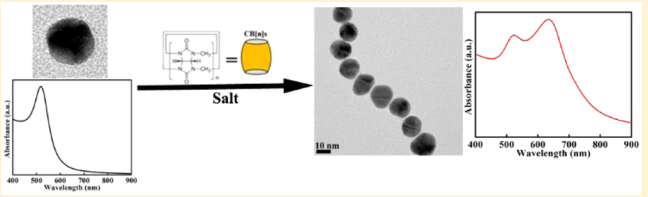

INTRODUCTION

Interactions (e.g., electrostatic, van der Waals, dipolar, and charge–dipole interactions) between nanostructures, as well as between nanostructures and linking elements, determine their dynamic behaviors, including stability and assembly, topology, and properties of nanostructures.[1−8] Establishing a novel approach to integrate nanoobjects into assemblies with better and predictable synthetic control and understanding of the interaction mechanism can be of significant benefit for engineering the topology and properties of assembled structures, as well as obtaining innovative applications and valuable insights into different interactions at nanoscale.[1,4,5,9−13] Several mechanisms and interactions have been reported to control the assembly of plasmonic nanostructures, which exhibit unique electronic, optical, and chemical properties, originating from the remarkable interplasmon coupling effects between the constituted components.[14] These assemblies find broad uses, especially in ultrasensitive chemical and biological sensing through colorimetry, surface-enhanced Raman scattering (SERS), etc. However, it is still difficult to induce assembly of nanoparticles (NPs) to generate one-dimensional (1D) nanostructures with subnanometer interparticle separation.

Here, engineering the exclusive and inclusive host–guest chemistry of cucurbit[*n*]urils (CB[*n*]s) is established to be a novel approach to modulate assembly of plasmonic NPs and stability of the assemblies in the solution. One-dimensional plasmonic nanochains with subnanometer interparticle separation can be generated. This work is important not only for achieving reproducible and controllable performance and structure of the assemblies in CB[*n*]s chemistry but also for providing new aspects of understanding and modulating the interaction between NPs and other supramolecular macrocycles, such as cyclodextrins, calixarenes, and pillar[*n*]arenes.[15] Strong synergistic effects will be trigged by the combination of plasmonic NP assemblies and outstanding host–guest chemical properties of CB[*n*]s, coupled with the ability to form stable host–guest exclusion and inclusion complexes with various guest molecules in aqueous media, which allows significant improvement in the performance of plasmonic NPs with many potential applications in sensing (e.g., SERS, colorimetric assistant ion detection and recognition), drug delivery, and catalysis.[15−20]

RESULTS AND DISCUSSION

Our strategy in this work was inspired by the unique structures and outstanding multiple recognition host–guest chemical properties of CB[*n*]s. CB[*n*] possesses a hydrophobic cavity, which is accessible through two polar carbonyl-laced and partially negatively charged portals (Figure 1a).[21] Formation of exclusion complexes from CB[*n*]s and cations (e.g., alkali metal

Received: July 16, 2016

DOI: 10.1021/acs.jpcc.6b07134
J. Phys. Chem. C XXXX, XXX, XXX−XXX

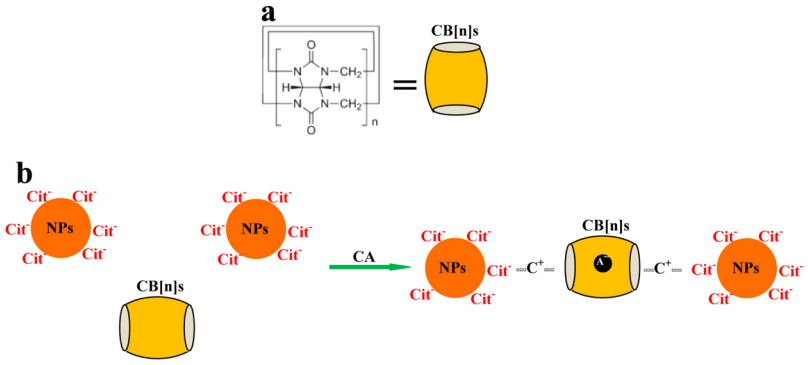

Figure 1. Schematic illustration of (a) CB[*n*] and (b) the assembly mechanism. CA, salt; C^+, cation; A^-, anion; Cit^-, citric anion.

ions, ammonium ions), via a combination of ion−dipole, hydrogen-bonding, and hydrophobic interactions between negatively charged carbonyl portals and cations, is expected.[15,17,18,22] In addition, the negatively charged surface of citrate-stabilized plasmonic NPs makes them highly attractive to oppositely charged species. On the basis of these principles, we recognized that it could be possible to modulate the exclusive host−guest chemistry via building a hinge (cations) to link the molecule bridge (CB[*n*]s) and plasmonic NPs to induce and tune assembly of NPs (Figure 1b). In contrast, the hydrophobic cavity renders CB[*n*]s good candidates as host molecules for various guest molecules, which can be encapsulated in CB[*n*]s.[15,23] Thus, far, the remarkably high selectivity of CB[*n*]s toward the shape and charge of a wide variety of guests with high association constants of host−guest inclusion complexes has been well established.[24,25] This exceptional inclusive host−guest chemical property promises an interesting possible way to manipulate the concentration of possible guests (e.g., anions) in the solution, which may influence the electrostatic interactions between cations and anions, giving another approach to engineer the assembly behavior of NPs (Figure 1b).[15,24]

Control of Exclusive Host−Guest Interaction. To validate the research ideas and achieve control over the assembly process of plasmonic NPs, three typical compositions of citrate-stabilized NPs—namely, Au, Ag, and AuAg alloy NPs—were selected as the prototypical systems and were prepared in our group.[26] Centrifugation was adopted to remove excess salt and citrate ions, and then the deposited NPs (namely, c-Au, c-Ag, c-$Au_{50}Ag_{50}$, and c-$Au_{25}Ag_{75}$ NPs) were redispersed into water. In this work, CB[5]s were chosen as a model. Monitoring the assembly process of NPs in the presence or absence of CB[5]s and/or additive salt was carried out by UV−vis spectroscopy, which was considered to be the most appropriate technique due to the surface plasmon resonance (SPR) of individual NPs and their assemblies. Transmission electron microscopy (TEM) was also employed to observe the tuned topological nanostructures.

For the first step, CB[5] solution (0.12 mM) with volume of 30 μL was added into the c-Au NP solution (2 mL, 16 nm diameter, as shown in Figure S1a). No obvious change could be determined comparing the absorption spectra and the color of the solutions with and without CB[5]s (Figure S1b and inset).[15,21,23,27] These results implied that no assembly of c-Au NPs was generated by use of CB[5]s alone, and this was confirmed by the TEM image (Figure S1c). In fact, even 50 μL of CB[5] solution could not lead to assembly of c-Au NPs.

The establishment of strong electrostatic attractive interaction between CB[*n*]s and alkali metal ions and formation of exclusion complex with positively charged surface, owing to coordination of the metal ions with the portal carbonyl oxygen atoms, suggest that alkali metal cations may act as an effective hinge to link the two negatively charged components, citrate-functionalized c-Au NPs and CB[*n*]s, as illustrated in Figure 1b.[28−30] In this case, two typical alkali metal ions, Na^+ and K^+, were chosen as the positively charged hinges. Figure 2a shows

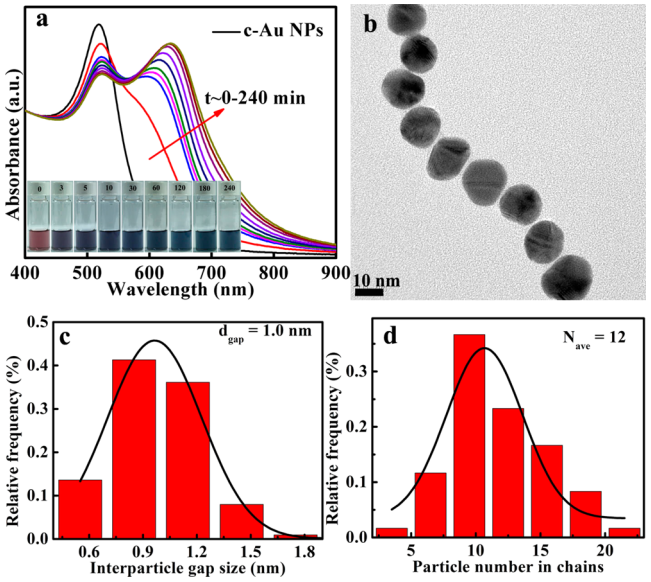

Figure 2. (a) Absorption spectra of c-Au NPs (16 nm) and c-Au NPs with addition of NaCl (30 μL) in the presence of CB[5]s after different incubation time: 0, 3, 5, 10, 30, 60, 120, 180, and 240 min. (Inset) Corresponding optical images of the solution. (b) Typical TEM image of assemblies (240 min). (c) Interparticle gap size distribution. (d) Particle number in nanochains.

the absorption spectra upon addition of 30 μL of NaCl (120 mM) into the CB[5]/c-Au NP (30 μL/2 mL) solution. Decrease of absorbance at 519 nm and a red shift from 519 to 524 nm are observable, which are assigned to assembly formation and the subsequent screening of the electrostatic repulsion.[4] A broad absorption band above 600 nm arises and evolves to become stronger with increasing incubation time and nearly stable after 2 h, which is accompanied by an obvious color change of the solution from red to blue (inset, Figure 2a). The appearance of a new absorption band at longer wavelength can be explained by dipole coupling between the plasmons of

DOI: 10.1021/acs.jpcc.6b07134
J. Phys. Chem. C XXXX, XXX, XXX−XXX

NPs, which is indicative of generation of 1D chainlike nanostructures, confirmed by the TEM image (Figure 2b).[4,5,31] The average gap between NPs is about 1 nm as determined from the TEM image (Figure 2c), and this verifies the possibility to generate subnanometer interparticle gaps in plasmonic assemblies.[17,18] This clearly indicates that the presence of NaCl triggers Au NP assembly in the CB[5]/c-Au NP solution. More TEM images under different magnifications were provided to confirm the production of 1D Au assemblies, as shown in Figure S2, which also implied that nearly all the Au NPs were assembled into chainlike structures. The average number in each chain is determined to be about 12, as displayed in Figure 2d. As expected, less NaCl induced smaller assemblies, as demonstrated by absorption spectra (Figure S3a), optical images (inset, Figure S3a), and TEM image (Figure S3b). In this case, some monodispersed Au NPs could be seen. A weak plasmon coupling band is seen, confirming that the presence of NaCl plays an important role in the assembly process of Au NPs. These also imply the possibility to control the length of the nanochains. To verify that the Na^+ ions, not the Cl^-, are responsible for the assembly behaviors, a control experiment adopting $NaNO_3$ under identical conditions was carried out. Generation of assemblies was confirmed by the absorption spectra (Figure S4a). In this case, the new peak increases more slowly and is weaker, together with a smaller shift (3 nm) of the single-particle SPR peak, than that with NaCl. These results evidence that Na^+ ions can induce assembly of Au NPs in the presence of CB[5]s and that anions may also affect the resulting assembly dynamic behaviors, for which more discussion will be given. Furthermore, our experiments confirmed that the generation of chainlike structures was reproducible, and the stability of the absorption behavior showed that the generated nanostructures could be stable for at least several hours. To reveal the potentially reversible nature of the assembly, we diluted the assembly solution with water (2 mL), and the blue color became a little weaker, but no other obvious color change could be seen, which showed that the process was irreversible and confirmed by the absorption spectrum (Figure S5).

Previous reports suggested that larger-sized K^+ could coordinate to the carbonyl oxygen atoms and cover the CB[5] portals more efficiently, subsequently interacting with CB[5]s more strongly than Na^+, which implies the possibility of causing faster assembly of Au NPs by use of K^+.[24,32,33] This proposal is validated by the fact that the coupling plasmonic band is much stronger and evolves more quickly after addition of KCl (Figure 3a), accompanied by an immediate color change from red to blue. Significant decrease of the peak at 519 nm with a large red shift of 13 nm (after 240 min) can be determined. Furthermore, in this case, the assemblies were not stable and precipitation happened in less than 1 h. The distinguishing difference can also be seen from the different ratios ($r = I_{p2}/I_{p1}$) of the coupling plasmonic band intensity (I_{p2}) to that of the individual particle SPR (I_{p1}), as revealed in Figure 3b, which is dependent on the length of the chains. In the presence of NaCl, r increases rapidly from ~0.4 to ~0.9 in 10 min and keeps nearly constant (~1.16) after 120 min, whereas r reaches about 1.49 and decreases after addition of KCl in 3 min, which also indicates that the generated assemblies are larger and unstable. In comparison, without CB[5]s no assembly occurred, as displayed in Figure S6, and this confirmed that increasing ion strength of the solution was not responsible for the assembly of NPs. Furthermore, as it is proposed that CB[5]s act as bridges to build the 1D assemblies, more CB[5]s should lead to more efficient assembly, which is consistent with the experimental result upon adding 40 μL of CB[5]s solution, as displayed in Figure S7. These results and discussions indicated that the proper amount of salt and CB[n]s is significantly important for generation of stable 1D assemblies as well as for controlling the chain length.

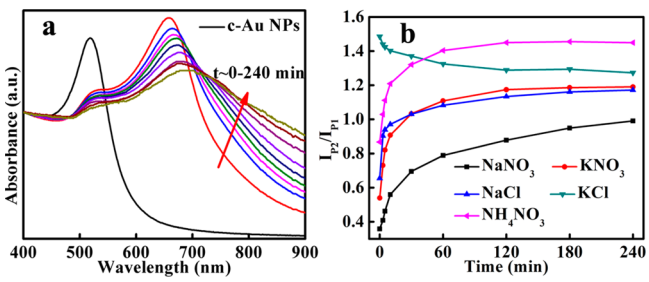

Figure 3. (a) Absorption spectra of c-Au NPs (16 nm) with addition of 30 μL of KCl. (b) r (= I_{p2}/I_{p1}) upon addition of $NaNO_3$, NaCl, KNO_3, KCl, and NH_4NO_3 after different incubation times.

These results imply that the controllable assembly of Au NPs can be obtained by modulating exclusive host–guest interaction. The suggested proposal was further evaluated by another control experiment, based on the inspiration that efficient coordination between the positively charged hinges and negatively charged CB[5]s before addition to the Au NP solution may facilitate the formation of assembly. To verify this suggestion, we prepared a mixture (1/1 v/v) of CB[5]s and NaCl to let them interact efficiently at first. Immediate assembly of Au NPs was caused by using this mixture solution, as demonstrated in Figure S8a. The assemblies were unstable and precipitated quickly from solution, confirmed by the decrease of r with increasing incubation time (Figure S8b). The faster assembly and higher ratios, compared to those for adding NaCl into the CB[5]/c-Au NP solution, evidence our suggestion.

Control of Inclusive Host–Guest Interaction. As discussed above, CB[n]s exhibit excellent host–guest chemical properties with high selectivity toward the shape and charge of various guests, which can be encapsulated in the cavity with high association constants of host–guest inclusion complexes. For instance, chlorine anions could be encapsulated in CB[5]s more easily to form molecular capsules than nitrate, owing to the smaller size of Cl^-.[34,35] This selective inclusive host–guest chemistry toward different anions prompts us to another interesting approach to engineer the assembly of Au NPs and the topological structures of the assemblies. This idea is supported by the aforementioned fact that NaCl leads to more pronounced assembly effects than $NaNO_3$. To further confirm the validity of our proposed technique, KNO_3 was tested to control the assembly of c-Au NPs. The absorption spectra (Figure S4b) exhibit a weaker and more slowly growing coupling SPR peak and a smaller red shift (3 nm) of the individual SPR peak, compared with Figure 3a, suggesting that KNO_3 caused assembly much less efficiently than KCl did. As there are always competing interactions between different species with negatively charged species and cationic ions, the electrostatic interactions between cations and anions from the salt may shield cations to weaken their ion–dipole interaction with CB[5]s and/or c-Au NPs, slowing down the assembly. Therefore, the encapsulation of Cl^- in the cavity of CB[5]s

DOI: 10.1021/acs.jpcc.6b07134
J. Phys. Chem. C XXXX, XXX, XXX–XXX

attributed to the host−guest chemistry effects will result in a decrease of Cl^- surrounding the cations, which weakens the "protective" shielding. Furthermore, the hydrogen bonds between counteranions and coordinated water molecules around cations can also be reduced.[36] Consequently, stronger electrostatic interactions between CB[5]s and cations accompanied by more pronounced assembly is expected. To further evaluate this principle, we switched to sodium hydrogen phosphate (Na_2HPO_4) and sodium sulfate (Na_2SO_4), whose anions, HPO_4^{2-} and SO_4^{2-}, are too big to be encapsulated in the cavity of CB[5]s.[37−39] Figure S9a shows the absorption spectra of Au NPs with increasing incubation time after injection of Na_2HPO_4 solution. The peak above 600 nm is weaker than that in the presence of NaCl with the same Na^+ concentration. Especially, much weaker plasmon coupling resonance is seen after addition of Na_2SO_4, as revealed in Figure S9b. Another control experiment was also performed with CB[7]s, whose cavity is bigger than the radius of SO_4^{2-}. We found that fast assembly occurred, assisted by SO_4^{2-}, as demonstrated in Figure 4a, with an intense coupling peak above

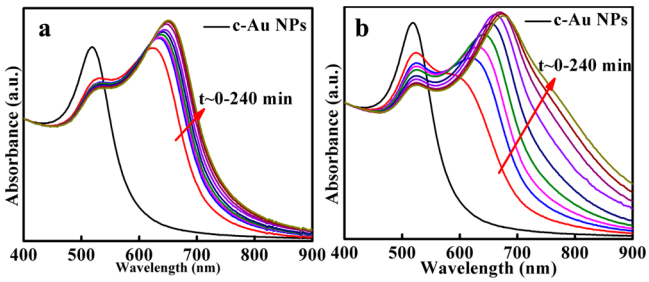

Figure 4. (a) Absorption spectra of c-Au NPs (16 nm) with addition of Na_2SO_4 in the presence of CB[7]s. (b) Absorption spectra of c-Au NPs with addition of 30 μL of CB[5]s followed by 30 μL of NH_4NO_3.

600 nm rapidly appearing and large *r*. In addition, another interesting phenomenon is worth noting: though *r* is large, no precipitation was observed after 4 h, indicating high stability of the assemblies. These results verify that the interaction between anions and cavity of CB[*n*]s plays an important role in inducing assembly of plasmonic NPs, and regulation of inclusive host−guest chemistry offers an effective strategy to tailor the assembly of Au NPs and their stability.

Control of Stability of the Assemblies. We further examined another type of bigger-sized cation, ammonium ion, which can interact with the negatively charged portals through not only charge−dipole but also hydrogen-bonding interactions, resulting in a larger enthalpy gain and in turn higher binding affinity between ammonium ions and CB[5]s than that between Na^+ or K^+ ions and CB[5]s.[15,40] Therefore, it can be predicted that NH_4^+ will induce assembly more efficiently. Figure 4b displays the absorption spectra of Au NPs in the presence of NH_4^+ (NH_4NO_3). Obvious assembly is observed with larger *r* (Figure 3b) than that in the presence of Na^+ or K^+, consistent with the proposed mechanism. In addition, the assembly was slower than with KCl, which confirmed that inclusive host−guest interaction played an important role in the induced assembly process of Au NPs. Furthermore, although *r* was larger than with KCl after about 2 h, the assemblies were stable and no aggregation was found after 4 h, which suggested that stability manipulation was allowed via controlling the host−guest chemistry.

Taken together, the fact that from Na^+ to K^+ and then to NH_4^+ the interaction between cations and CB[5]s becomes stronger, resulting in faster and more efficient assembly, and the determination of significant difference of the assembly behaviors induced by CB[5]/Na_2SO_4 and CB[7]/Na_2SO_4, as well as by CB[5]/$NaNO_3$ and CB[5]/Na_2SO_4, clearly support the proposed mechanism in Figure 1b. The data unambiguously show the possibility of managing assembly of Au NPs and the topological structures and properties of assemblies by modulating host−guest chemistry.

Assembly Control of Nanoparticles with Different Sizes and Compositions. Our methodology for assembly management via control of host−guest chemistry is potentially broadly applicable to Au NPs and other plasmonic NPs with different sizes. In order to confirm the generality, by use of 30 nm c-Au NPs, as observed in Figure S10a, significant and fast assembly can be determined, and 1D Au nanochains were displayed in Figure S10b. Here, the position of plasmonic peak P_2 is around 714 nm, which indicates that the coupling plasmonic optical response is tunable with adjusted conditions, such as particle size. We further examined other NPs (e.g., Ag NPs and $Au_{50}Ag_{50}$ and $Au_{25}Ag_{75}$ alloy NPs), whose optical performance is also extremely sensitive to their aggregation state. Significantly, we observed an obvious color change with the addition of CB[5]s and NaCl. As typical examples, dipole coupling plasmon peaks corresponding to 1D nanochains were observed. One-dimensional nanochains consisting of c-Ag, c-$Au_{50}Ag_{50}$, and c-$Au_{25}Ag_{75}$ alloy NPs are shown in Figure 5panels a−c, respectively. We confirmed that CB[5]s or NaCl

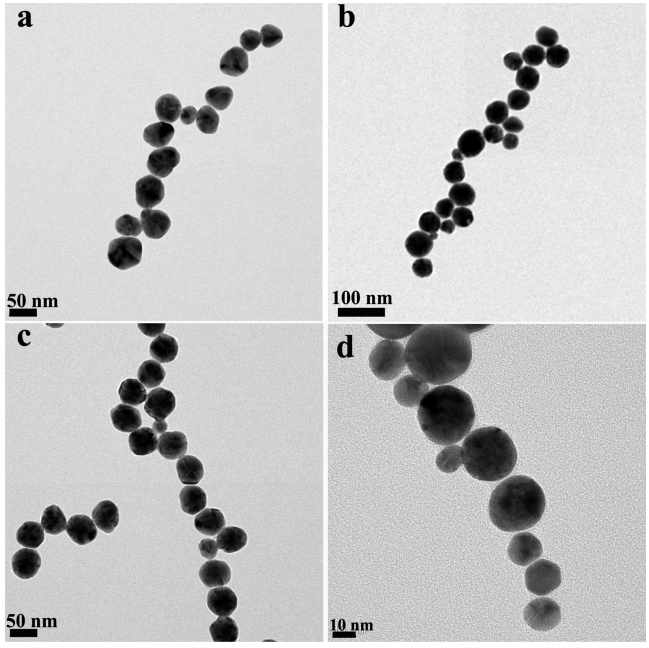

Figure 5. c-Au NP nanochains: (a) 36 nm c-Ag, (b) 44 nm c-$Au_{50}Ag_{50}$, (c) 50 nm c-$Au_{25}Ag_{75}$, and (d) 16/30 nm.

alone could not induce assembly of Ag or AuAg alloy NPs. One-dimensional plasmonic nanochains can also be synthesized from NPs with different sizes. As revealed in Figure 5d, 1D NP assembly constructed of c-Au NPs with size of 16 and 30 nm can be observed.

Simulation of Optical Response of One-Dimensional Au Nanoparticle Chains. To understand further the optical

DOI: 10.1021/acs.jpcc.6b07134
J. Phys. Chem. C XXXX, XXX, XXX−XXX

properties determined in experiments, we performed simulations of the optical response of 1D Au NP chains. We began by considering a linear chain consisting of Au NPs with diameter 16 nm, separated by a 1 nm interparticle gap (l_{gap} = 1 nm) and illuminated by an unpolarized plane wave (orthogonal to the chain). A strong coupling plasmon resonance peak in the nanochain is seen in Figure 6a, which confirms the

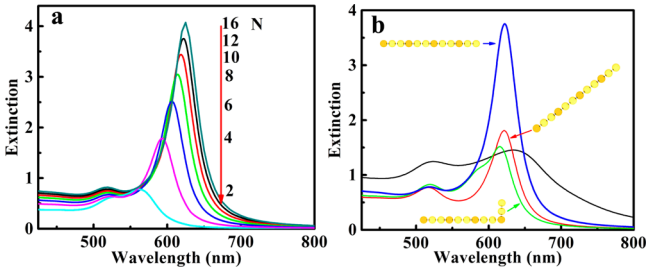

Figure 6. (a) Calculated extinction spectra of 1D Au (16 nm) nanochains with different particle numbers. (b) Experimental (black line, Figure 2a, 4 h) and simulated extinction spectra of 1D Au (16 nm) NP nanochain with N = 12 (l_{gap} = 1 nm). Blue line, linear chain orthogonal to the unpolarized plane wave; red line, influence on extinction spectra of nanochain random spatial orientation (θ = 0–90°); green line, additional influence of nanochain nonlinearity on extinction spectra.

experimental results. Figure S11 shows that increasing Au NP number (N) from 2 to 16 results in a red shift of the coupling peak (P_2) position. Furthermore, when the number reaches about 12–16, the resonance red shift is small and nearly saturates.[41] To explore potential ways to tailor the optical response of NP chains by introducing additional degrees of freedom, we also checked the effect of the interparticle gap (l_{gap}). In this case, the particle number was set to 12. The Au nanochain exhibits a large red shift in extinction spectra with decreasing interparticle gap (Figure S12). This behavior confirms the importance of controlling the interparticle gap in plasmonic assemblies, as stated previously and provided here for instance by the CB[n]s. We also checked the optical response of nonlinear nanochains, as well as the effect of relative angle (θ) between the chains and the irradiated light electric field. Figure S13a indicates that a small blue shift may be caused by the shape change from linear to nonlinear. Furthermore, the coupling peak becomes weaker and broader when the direction relationship between the irradiated light electric field and chain axis changes from parallel (θ = 0°) to nonparallel ($\theta \neq 0°$), and disappears when θ = 90°, as displayed in Figure S13b. A comparison analysis between experimental and simulation results was carried out further, as revealed in Figure 6b. After the effect of nonlinearity and spatial rotation (θ = 0–90°) was considered, the simulation extinction (green line) is much closer to the experimental result, with a small blue shift (ΔP_1 = 5 nm, and ΔP_2 = 20 nm) compared to the experimental absorption. Several reasons may cause this discrepancy, for example, simplification of the simulation model and change of the dielectric function in the solution due to the presence of salt and CB[n]s. The discrepancy also implies that the realistic structure of the nanochains is more complicated that the linear case, as shown in Figure 2b and Figure S2.

Discussions. The previous report showed that cucurbit[n]urils (CB[n]s) can induce assembly of Au NPs to generate aggregation.[17] However, there has been little effort to control the assembly and the mechanism has not been well revealed. Therefore, it is still a grand challenge to gain better control and understanding of the induced self-assembly behaviors, which are significant issues lying at the heart of supramolecular macrocycle–nanoparticle science. Furthermore, our controlled experiments showed that CB[n] or salt does not necessarily induce assembly of aggregation under certain conditions. There have been no reports about engineering the host–guest interactions of CB[n]s to tune the assembly of plasmonic NPs. Here, we demonstrated that the exclusive and inclusive interactions between CB[n]s and different salt ions provide a versatile and general method to tune the assembly of Au NPs, along with controlling the stability of the assemblies in the solution. Our results promise a new concept and mechanism to tune the assembly of plasmonic NPs in but beyond the supramolecular chemistry.

CONCLUSION

In summary, we have demonstrated simultaneously managing assembly of plasmonic NPs with controllable size and composition and stability of these assemblies by engineering the exclusive and inclusive host–guest chemistry of CB[n]s with the assistance of selected salts. One-dimensional plasmonic nanochains with a rigid subnanometer interparticle gap were formed, which exhibited strong tunable dipole coupling between the NPs. Detailed discussions and comparison with simulation investigations have been performed to study the structure and plasmonic coupling properties of the 1D nanochains. We note that the proposed strategy can be general and facile to be potentially applied to many positively charged NPs to engineer a wide range of material properties such as optical and electrical characteristics, where the particle coupling is essential. This work contributes not only to the tunable assembly of plasmonic NPs but also to fundamental understanding of the host–guest chemistry of CB[n]s, as well as providing useful information for their applications.

EXPERIMENTAL SECTION

Methods. *Synthesis of Gold Nanoparticles (16 nm).* Au NPs with size of 16 nm were fabricated by the standard citrate reduction of hydrogen tetrachloroaurate(III). Typically, 0.5 mL of $HAuCl_4$ solution (30 mM) was injected into boiling H_2O (50 mL), followed by injection of 0.5 mL of sodium citrate solution (120 mM). After boiling for 15 min under vigorous stirring, Au NPs were separated by centrifugation (14 000 rpm/min, 10 min). The deposited Au NPs were redispersed into water.

Synthesis of Au (30 nm), Ag, $Au_{50}Ag_{50}$, and $Au_{25}Ag_{75}$ Nanoparticles. Au (30 nm), Ag, $Au_{50}Ag_{50}$, and $Au_{25}Ag_{75}$ NPs were synthesized by a seeded growth method developed by our group.[26]

Control of Assembly of Au Nanoparticles with Addition of CB[5]s and Salt. To control the assembly, typically, 30 μL of CB[5]s aqueous solution (0.12 mM, Sigma–Aldrich) was added into 2 mL of Au NPs solution (30 μL/2 mL), and the solution was shaken to let it reach equilibrium. Then 30 μL of NaCl solution (120 mM) was injected into the above mixture, and slight shaking was performed for about 3 s to allow it to be homogeneous.

Characterization. Absorption spectra were acquired with an Epoch spectrophotometer (Biotek). TEM images were

DOI: 10.1021/acs.jpcc.6b07134
J. Phys. Chem. C XXXX, XXX, XXX–XXX

recorded by a high-resolution transmission electron microscope (JEOL, JEM2010F).

Calculations. All of the theoretical results are obtained by numerical simulations based on extended Mie theory.[42]

■ ASSOCIATED CONTENT

Supporting Information

The Supporting Information is available free of charge on the ACS Publications website at DOI: 10.1021/acs.jpcc.6b07134.

Thirteen figures showing size distribution, absorption spectra, and TEM image of c-Au NPs; TEM images of assemblies; absorption spectra of c-Au NPs with addition of NaCl, $NaNO_3$, KNO_3, KCl, CB[5]s, CB[5]s/NaCl mixture, Na_2HPO_4, and Na_2SO_4; P_2 positions of 1D Au nanochains with different particle numbers and interparticle gaps; extinction spectra and P_2 position of 1D Au nanochains with different interparticle gaps, shapes, and rotation angles (PDF)

■ AUTHOR INFORMATION

Corresponding Author

*E-mail michel.meunier@polymtl.ca.

Present Address

§(D.T.) Institute of Advanced Energy, Kyoto University, Uji, Kyoto 611-0011, Japan.

Author Contributions

D.T. conceived and designed the experiments and wrote the paper. D.T. and S.T. prepared the plasmonic NPs. Y.Y., D.R., and M.M. provided insightful discussions. S.P. performed the simulation.

Notes

The authors declare no competing financial interest.

■ ACKNOWLEDGMENTS

D.T. acknowledges financial support from the postdoctoral Groupe de Recherche en Sciences et Technologies Biomédicales scholarship (2014−2015). We thank Yves Drolet for technical support.

■ REFERENCES

(1) Alivisatos, A. P. Semiconductor Clusters, Nanocrystals, and Quantum Dots. *Science* **1996**, *271*, 933−937.

(2) Henzie, J.; Grünwald, M.; Widmer-Cooper, A.; Geissler, P. L.; Yang, P. Self-Assembly of Uniform Polyhedral Silver Nanocrystals into Densest Packings and Exotic Superlattices. *Nat. Mater.* **2012**, *11*, 131−137.

(3) Wasio, N. A.; Quardokus, R. C.; Forrest, R. P.; Lent, C. S.; Corcelli, S. A.; Christie, J. A.; Henderson, K. W.; Kandel, S. A. Self-Assembly of Hydrogen-Bonded Two-Dimensional Quasicrystals. *Nature* **2014**, *507*, 86−89.

(4) Ojea-Jiménez, I.; Puntes, V. Instability of Cationic Gold Nanoparticle Bioconjugates: the Role of Citrate Ions. *J. Am. Chem. Soc.* **2009**, *131*, 13320−13327.

(5) Zhang, H.; Wang, D. Controlling the Growth of Charged-Nanoparticle Chains through Interparticle Electrostatic Repulsion. *Angew. Chem., Int. Ed.* **2008**, *47*, 3984−3987.

(6) Han, X.; Goebl, J.; Lu, Z.; Yin, Y. Role of Salt in the Spontaneous Assembly of Charged Gold Nanoparticles in Ethanol. *Langmuir* **2011**, *27*, 5282−5289.

(7) Volkert, A. A.; Subramaniam, V.; Ivanov, M. R.; Goodman, A. M.; Haes, A. J. Salt-Mediated Self-Assembly of Thioctic Acid on Gold Nanoparticles. *ACS Nano* **2011**, *5*, 4570−4580.

(8) Stoffelen, C.; Munirathinam, R.; Verboom, W.; Huskens, J. Self-Assembly of Size-Tunable Supramolecular Nanoparticle Clusters in a Microfluidic Channel. *Mater. Horiz.* **2014**, *1*, 595−601.

(9) Warner, M. G.; Hutchison, J. E. Linear Assemblies of Nanoparticles Electrostatically Organized on DNA Scaffolds. *Nat. Mater.* **2003**, *2*, 272−277.

(10) Gutowska, A.; Li, L.; Shin, Y.; Wang, C. M.; Li, X. S.; Linehan, J. C.; Smith, R. S.; Kay, B. D.; Schmid, B.; Shaw, W.; Gutowski, M.; Autrey, T. Nanoscaffold Mediates Hydrogen Release and the Reactivity of Ammonia Borane. *Angew. Chem., Int. Ed.* **2005**, *44*, 3578−3582.

(11) Lin, S.; Li, M.; Dujardin, E.; Girard, C.; Mann, S. One-Dimensional Plasmon Coupling by Facile Self-Assembly of Gold Nanoparticles into Branched Chain Networks. *Adv. Mater.* **2005**, *17*, 2553−2559.

(12) Pyun, J. Self-Assembly and Colloidal Polymerization of Polymer-Nanoparticle Hybrids into Mesoscopic Chains. *Angew. Chem., Int. Ed.* **2012**, *51*, 12408−12409.

(13) Ohya, Y.; Miyoshi, N.; Hashizume, M.; Tamaki, T.; Uehara, T.; Shingubara, S.; Kuzuya, A. Formation of 1D and 2D Gold Nanoparticle Arrays by Divalent DNA-Gold Nanoparticle Conjugates. *Small* **2012**, *8*, 2335−2340.

(14) Grzelczak, M.; Vermant, J.; Furst, E. M.; Liz-Marzán, L. M. Directed Self-Assembly of Nanoparticles. *ACS Nano* **2010**, *4*, 3591−3605.

(15) Montes-García, V.; Pérez-Juste, J.; Pastoriza-Santos, I.; Liz-Marzán, L. M. Metal Nanoparticles and Supramolecular Macrocycles: A Tale of Synergy. *Chem. - Eur. J.* **2014**, *20*, 10874−10883.

(16) An, Q.; Li, G.; Tao, C.; Li, Y.; Wu, Y.; Zhang, W. A General and Efficient Method to Form Self-Assembled Cucurbit[n]uril Monolayers on Gold Surfaces. *Chem. Commun.* **2008**, 1989−1991.

(17) Taylor, R. W.; Lee, T.-C.; Scherman, O. A.; Esteban, R.; Aizpurua, J.; Huang, F. M.; Baumberg, J. J.; Mahajan, S. Precise Subnanometer Plasmonic Junctions for SERS within Gold Nanoparticle Assemblies using Cucurbit[n]uril " Glue. *ACS Nano* **2011**, *5*, 3878−3887.

(18) Kasera, S.; Biedermann, F.; Baumberg, J. J.; Scherman, O. A.; Mahajan, S. Quantitative SERS using the Sequestration of Small Molecules inside Precise Plasmonic Nanoconstructs. *Nano Lett.* **2012**, *12*, 5924−5928.

(19) Zheng, Y.; Yu, Z.; Parker, R. M.; Wu, Y.; Abell, C.; Scherman, O. A. Interfacial Assembly of Dendritic Microcapsules with Host-Guest Chemistry. *Nat. Commun.* **2014**, *5*, No. 5772.

(20) Kim, C.; Agasti, S. S.; Zhu, Z.; Isaacs, L.; Rotello, V. M. Recognition-Mediated Activation of Therapeutic Gold Nanoparticles inside Living Cells. *Nat. Chem.* **2010**, *2*, 962−966.

(21) Masson, E.; Ling, X.; Joseph, R.; Kyeremeh-Mensah, L.; Lu, X. Cucurbituril Chemistry: a Tale of Supramolecular Success. *RSC Adv.* **2012**, *2*, 1213−1247.

(22) Ni, X. L.; Xiao, X.; Cong, H.; Zhu, Q. J.; Xue, S. F.; Tao, Z. Self-Assemblies Based on the "Outer-Surface Interactions" of Cucurbit[n]urils: New Opportunities for Supramolecular Architectures and Materials. *Acc. Chem. Res.* **2014**, *47*, 1386−1395.

(23) Lagona, J.; Mukhopadhyay, P.; Chakrabarti, S.; Isaacs, L. The Cucurbit[n]uril Family. *Angew. Chem., Int. Ed.* **2005**, *44*, 4844−4870.

(24) Ni, X. L.; Xiao, X.; Cong, H.; Liang, L. L.; Cheng, K.; Cheng, X. J.; Ji, N. N.; Zhu, Q. J.; Xue, S. F.; Tao, Z. Cucurbit[n]uril-Based Coordination Chemistry: from Simple Coordination Complexes to Novel Poly-Dimensional Coordination Polymers. *Chem. Soc. Rev.* **2013**, *42*, 9480−9508.

(25) Yu, Z.; Zhang, J.; Coulston, R. J.; Parker, R. M.; Biedermann, F.; Liu, X.; Scherman, O. A.; Abell, C. Supramolecular Hydrogel Microcapsules via Cucurbit[8]uril Host-Guest Interactions with Triggered and UV-Controlled Molecular Permeability. *Chem. Sci.* **2015**, *6*, 4929−4933.

(26) Rioux, D.; Meunier, M. Seeded Growth Synthesis of Composition and Size-Controlled Gold-Silver Alloy Nanoparticles. *J. Phys. Chem. C* **2015**, *119*, 13160−13168.

(27) Cao, M.; Lin, J.; Yang, H.; Cao, R. Facile Synthesis of Palladium Nanoparticles with High Chemical Activity using Cucurbit[6]uril as Protecting Agent. *Chem. Commun.* **2010**, *46*, 5088−5090.
(28) Buschmann, H.-J.; Cleve, E.; Jansen, K.; Wego, A.; Schollmeyer, E. Complex Formation between Cucurbit[n]urils and Alkali, Alkaline Earth and Ammonium Ions in Aqueous Solution. *J. Inclusion Phenom. Mol. Recognit. Chem.* **2001**, *40*, 117−120.
(29) Kim, Y.; Kim, H.; Ko, Y. H.; Selvapalam, N.; Rekharsky, Y. M.; In-oue, V. O.; Kim, K. Complexation of Aliphatic Ammonium Ions with a Water-Soluble Cucurbit[6]uril Derivative in Pure Water: Isothermal Calorimetric, NMR, and X-ray Crystallographic Study. *Chem. - Eur. J.* **2009**, *15*, 6143−6151.
(30) Lee, J. W.; Samal, S.; Selvapalam, N.; Kim, H.-J.; Kim, K. Cucurbituril Homologues and Derivatives: New Opportunities in Supramolecular Chemistry. *Acc. Chem. Res.* **2003**, *36*, 621−630.
(31) Lee, T. C.; Scherman, O. A. A Facile Synthesis of Dynamic Supramolecular Aggregates of Cucurbit[n]uril (n = 5−8) Capped with Gold Nanoparticles in Aqueous Media. *Chem. - Eur. J.* **2012**, *18*, 1628−1633.
(32) Jeon, Y. M.; Kim, J.; Whang, D.; Kim, K. Molecular Container Assembly Capable of Controlling Binding and Release of Its Guest Molecules: Reversible Encapsulation of Organic Molecules in Sodium Ion Complexed Cucurbituril. *J. Am. Chem. Soc.* **1996**, *118*, 9790−9791.
(33) Heo, J.; Kim, J.; Whang, D.; Kim, K. Columnar One-Dimensional Coordination Polymer Formed with a Metal Ion and a Host-Guest Complex as Building Blocks: Potassium Ion Complexed Cucurbituril. *Inorg. Chim. Acta* **2000**, *297*, 307−312.
(34) Liu, J. X.; Long, L. S.; Huang, R. B.; Zheng, L. S. Molecular Capsules Based on Cucurbit[5]uril Encapsulating "Naked" Anion Chlorine. *Cryst. Growth Des.* **2006**, *6*, 2611−2614.
(35) Liu, J.-X.; Long, L.-S.; Huang, R.-B.; Zheng, L.-S. Interesting Anion-Inclusion Behavior of Cucurbit[5]uril and Its Lanthanide-Capped Molecular Capsule. *Inorg. Chem.* **2007**, *46*, 10168−10173.
(36) Lü, J.; Lin, J. X.; Cao, M. N.; Cao, R. Cucurbituril: a Promising Organic Building Block for the Design of Coordination Compounds and Beyond. *Coord. Chem. Rev.* **2013**, *257*, 1334−1356.
(37) Thuéry, P.; Masci, B. Uranyl Ion Complexation by Cucurbiturils in the Presence of Perrhenic, Phosphoric, or Polycarboxylic Acids. Novel Mixed-Ligand Uranyl-Organic Frameworks. *Cryst. Growth Des.* **2010**, *10*, 716−725.
(38) Fawcett, W. R. Charge Distribution Effects in the Solution Chemistry of Polyatomic Ions. *Condens. Matter Phys.* **2005**, *8*, 413−424.
(39) Manku, G. S. *Theoretical Principles of Inorganic Chemistry*; Tata McGraw-Hill: New Delhi, 1980; Chapt. 3, p 102.
(40) Rueda-Zubiaurre, A.; Herrero-García, N.; del Rosario Torres, M.; Fernández, I.; Barcina, J. O. Rational Design of a Nonbasic Molecular Receptor for Selective NH^{4+}/K^{+} Complexation in the Gas Phase. *Chem. - Eur. J.* **2012**, *18*, 16884−16889.
(41) Tserkezis, C.; Taylor, R. W.; Beitner, J.; Esteban, R.; Baumberg, J. J.; Aizpurua, J. Optical Response of Metallic Nanoparticle Heteroaggregates with Subnanometric Gaps. *Part. Part. Syst. Charact.* **2014**, *31*, 152−160.
(42) Xu, Y. L. Electromagnetic Scattering by an Aggregate of Spheres. *Appl. Opt.* **1995**, *34*, 4573−4588.

DOI: 10.1021/acs.jpcc.6b07134
J. Phys. Chem. C XXXX, XXX, XXX−XXX